Journal of Alloys and Compounds 527 (2012) 204–209

Contents lists available at SciVerse ScienceDirect

Journal of Alloys and Compounds

journal homepage: www.elsevier.com/locate/jallcom

Improvement of thermoelectric properties of WO_3 ceramics by ZnO addition

Haiqing Wang[a,*], Xiang Dong[b], Shujie Peng[a], Liang Dong[b], Yu Wang[b]

[a] School of Materials Science and Engineering, Southwest Jiaotong University, Chengdu, Sichuan 610031, China
[b] School of Electrical Engineering, Southwest Jiaotong University, Chengdu, Sichuan 610031, China

ARTICLE INFO

Article history:
Received 19 September 2011
Received in revised form 2 March 2012
Accepted 5 March 2012
Available online xxx

Keywords:
Electrical conductivity
Seebeck coefficient
WO_3 ceramics
Power factor
ZnO

ABSTRACT

The thermoelectric properties of tungsten trioxide (WO_3) ceramics doped with zinc oxide (ZnO) were investigated from 473 to 973 K. The results revealed that doping WO_3 with ZnO could promote the grain growth and the densification. Moreover, the addition of ZnO into WO_3 obviously raised the electrical conductivity (σ) of the ceramics by about two orders of magnitude with only slightly decreasing its absolute value of the Seebeck coefficient ($|s|$). Thus, the magnitude of the power factor (σs^2) was enhanced tremendously by adding ZnO. In addition, there was a second phase ($ZnWO_4$) segregation at the grain boundaries in the samples containing more than 0.5 mol% ZnO, which inhibited the further grain growth and reduced the σ and $|s|$. Therefore, there existed an optimum doping concentration of ZnO in WO_3 for obtaining a better power factor.

1. Introduction

Thermoelectric materials have attracted considerable attention due to their ability to produce electric power from waste heat which can be used as a way of solving the global warming problem. Metal oxides have been exploited as candidates for applications in thermoelectric generation due to their better thermal and chemical stability at high temperatures than alloys. In 1997, Terasaki et al. [1] first reported a discovery of some layered p-type cobalt oxides, which have a comparable figure of merit to the conventional materials. Since then, attention has been focused on the metal oxides, and some oxides such as $NaCo_2O_4$ [2], $LaCoO_3$ [3,4] and ZnO [5–9] have been widely studied.

In recent years, some other metal oxides have received considerable attention as thermoelectric materials, such as $SrTiO_3$ [10–14], TiO_2 [15,16] and SnO_2 [17], the utilizations of which in the varistors and gas sensors are basically the same as ZnO. Among these novel thermoelectric oxides, $SrTiO_3$ with a cubic perovskite structure has been considered as a promising thermoelectric candidate for the n-type metal oxide because of its rather large Seebeck coefficient [14]. WO_3 is an n-type metal oxide with a perovskite-like structure and usually labeled as WO_{3-x} due to the oxygen deficiency [18]. The electronic structures of WO_3 are also similar to $SrTiO_3$ [19], and the applications of WO_3 in varistors and gas sensors usually have the same effects as $SrTiO_3$ [20–23]. Therefore, it would be interesting to investigate the thermoelectric properties of WO_3. We previously reported the thermoelectric properties of WO_3 doped with CeO_2 over the temperature range 323–673 K [24], and it was found that the addition of CeO_2 could densify the WO_3 ceramics to improve the thermoelectric characteristic. However, the electrical conductivity of the WO_3-based ceramics is quite low and the higher temperature thermoelectric properties of WO_3 have not been reported, and thus the thermoelectric properties of WO_3 require further improvement and research.

Previous study [24] implied that the densification of the WO_3-based ceramics was attributed to the increasing concentration of oxygen vacancies in the grain boundary region. The oxygen vacancies can be also introduced in the WO_3 ceramics by adding the ZnO to keep the charge neutrality when substituting the Zn^{2+} ion for the W^{6+}. Thus, the ZnO addition would also densify the WO_3 ceramics, and hence enhance the thermoelectric properties. In addition, there is an advantage using the ZnO instead of the CeO_2 that the ZnO is inexpensive and highly abundant relative to the CeO_2. Therefore, in the present study, we investigated the thermoelectric properties of WO_3 ceramics in a higher temperature range from 473 K to 973 K, and attempted to modify its thermoelectric characteristic by doping with ZnO.

2. Experimental procedures

Raw materials of analytical grade: WO_3 (purity ≥99.9%) and ZnO (purity ≥99.9%) were used to prepare the compositions of $(100-x)$ mol% WO_3 + x mol% ZnO, where x = 0.0, 0.1, 0.5, 1.0, 5.0 and 10.0. After milled with agate balls and ethanol for 10 h, the powders were then granulated with binder and pressed at 100 MPa to form discs 10 mm in diameter and 3 mm in thickness. The grain size of the ceramics has notable effects on its thermoelectric properties [25], and thus the green compacts were sintered in a new way to get a smaller grain size than our previous work [20–22]. In order to get a smaller grain size, the discs with the same concentration

* Corresponding author. Tel.: +86 028 87601134; fax: +86 028 87600787.
E-mail address: whq20054692@126.com (H. Wang).

0925-8388/$ – see front matter © 2012 Elsevier B.V. All rights reserved.
doi:10.1016/j.jallcom.2012.03.022

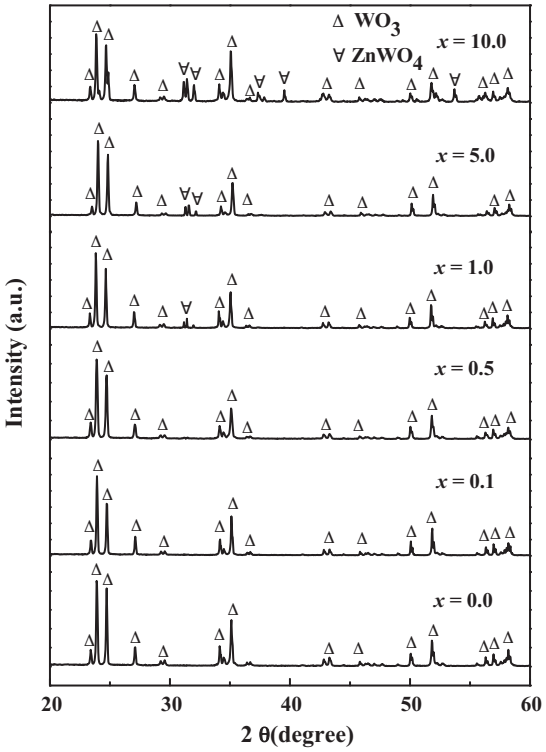

Fig. 1. XRD patterns of the $(100-x)$ mol% WO_3 + x mol% ZnO samples.

were sintered at 400 °C in air for 30 min, and then were sintered at 1100 °C for 2 h. The heating rate was maintained at 100 °C/h.

The microstructure of samples was examined using scanning electron microscopy (FEI QUANTA200 with an energy dispersive spectrometer). As for the SEM and EDX analysis, samples were cleaned in acetone, mounted, and gold-coated to prevent charging. Average grain sizes of the samples have been estimated by the line-intersecting method, given by [26]:

$$d = \frac{1.56L}{MN} \quad (1)$$

where d is the average grain size, L is the random line length on the micrograph, M is the magnification of the micrograph and N is the number of the grain boundaries intercepted by lines. The porosity of the specimens has been measured by the Archimedes principle. The crystalline phases of these sintered samples were identified by X-ray diffraction technologies (7602EA ALMELO) under the following experimental conditions: λ(Cu Kα) = 0.15406 nm, 40 kV, 40 mA, $20^\circ \le 2\theta \le 60^\circ$. The electrical conductivity from 473 K to 973 K was measured by means of a standard four-probe method using the KEITHLEY 2400. The thermoelectric power from 473 K to 973 K was calculated from the thermoelectric voltage collected with KEITHLEY 2400 and the temperature difference between the two ends of the sample.

3. Results and discussion

Fig. 1 illustrates the XRD patterns of the samples with different amount of ZnO. It is revealed that the major phase of the samples is a WO_3 phase, and there is an obvious second phase in the doped samples when the content of ZnO exceeds 0.5 mol%. The second phase is identified as $ZnWO_4$ (JCPDS file card number 15-0774) through the XRD analysis. The result is consistent with the previous study [27]. From the XRD patterns, the lattice parameters of the samples shown in Fig. 2 were obtained through the Jade 5.0 software by the Rietveld method [28]. At room temperature, WO_3 is monoclinic with lattice parameters a = 7.30 Å, b = 7.53 Å, c = 3.85 Å [19]. The values calculated by the structural refinement differ by no more than 2% from the theoretical values. The radius of W^{6+} (0.62 Å) is smaller than that of Zn^{2+} (0.74 Å) [29]. Thus, it can be observed from Fig. 2 that a-axis, c-axis and the unit cell volume lattice parameters tend to increase and b-axis lattice parameter decreases as the ZnO concentration increases to 1.0 mol%. Continuing increasing the ZnO concentration, the lattice parameters of the samples almost keep constant. According to the foregoing discussion, it can be concluded that the solid solutions $W_{1-x}Zn_xO_{3-y}$ are fabricated and the solubility limit of ZnO in WO_3 is between 0.5 and 1.0 mol% because of the almost unchanged lattice parameters and the formation of the second phase $ZnWO_4$.

Table 1
Average grain size and porosity of the samples with different ZnO contents.

ZnO (mol%)	Grain size (μm)	Porosity (%)
0.0	6.3	19.36
0.1	6.9	7.07
0.5	7.8	5.11
1.0	7.3	6.86
5.0	7.1	7.16
10.0	6.7	7.35

The SEM micrographs of the sintered WO_3 ceramics with different amount of ZnO are shown in Fig. 3. It can be seen that the densification of the doped ceramics are better than the pure one, and that the grain size of samples increases with the addition of ZnO in WO_3 up to 0.5 mol% and then decreases with more ZnO added. The rod-shaped structure can be evidently observed at the grain boundary regions as samples contain more than 1.0 mol% ZnO. As shown in Fig. 4, the EDX spectra of the rod-shaped structure for WO_3 ceramics doped with 5.0 mol% ZnO indicates that the Zn-rich phase exists between WO_3 grains. On the basis of the XRD analysis, the rod-shaped structure is a grain of $ZnWO_4$. Our previous researches suggested that the grain size of WO_3-based ceramics remained almost constant with an average grain size about 10 μm and that the open porosity was about 14% [20–24]. The grain size and the porosity of all samples in this research are given in Table 1. The grain size and the porosity lie in the range 6.3–7.8 μm and 5.11–19.36%, respectively. The grain size of the samples in this work is obviously smaller than our previous investigation. Although the grain size of the samples is a little bit enhanced by adding ZnO into WO_3, the porosity of the doped samples is extremely reduced. Therefore, doping WO_3 with ZnO can improve the mass transfer during sintering process, leading to the grain growth and the increasing densification.

Previous study [24] implied that the densification of the WO_3-based ceramics might be similar to the one that occurred in the SnO_2-based polycrystalline systems, which was attributed to the increasing concentration of oxygen vacancies in the grain boundary region [30–32]. The densifying mechanism of the WO_3–ZnO ceramics and the formation of oxygen vacancies could obey the following reactions:

$$ZnO \xrightarrow{WO_3} Zn_W'''' + 2V_O^{\bullet\bullet} + O_O^X \quad (2)$$

$$ZnO + WO_3 \rightarrow ZnWO_4 \quad (3)$$

Eq. (2) represents that the addition of ZnO into WO_3 leads to the creation of additional oxygen vacancies, which increase the flux of oxygen ions and promote the grain growth and the densification. Reaction (3) reveals the formation of the second phase, $ZnWO_4$, by the reaction of ZnO and WO_3 due to the content of ZnO in WO_3 above the solubility limit. The second phase $ZnWO_4$ lowers the grain boundary mobility through the solute drag mechanism during sintering process and enables the pores to stay attached to the moving grain boundaries. Therefore, the proper addition of ZnO can promote the grain growth and the densification of the WO_3-based ceramics. While the content of ZnO in WO_3 exceeds its solubility limit, the second phase $ZnWO_4$ segregates between the WO_3 grains reducing the process of the mass transport, and thus the densification of samples become worse with more ZnO doped.

As the electrical conductivity of samples is extremely improved through doping with ZnO, the curves of $\log_{10}\sigma$ against T are shown

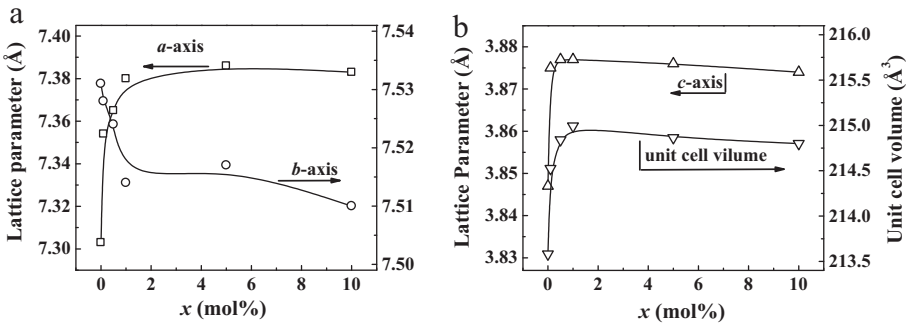

Fig. 2. Lattice parameters of the undoped and ZnO-doped WO_3, (a) *a*-axis and *b*-axis, (b) *c*-axis and unit cell volume plotted in terms of ZnO additive concentrations.

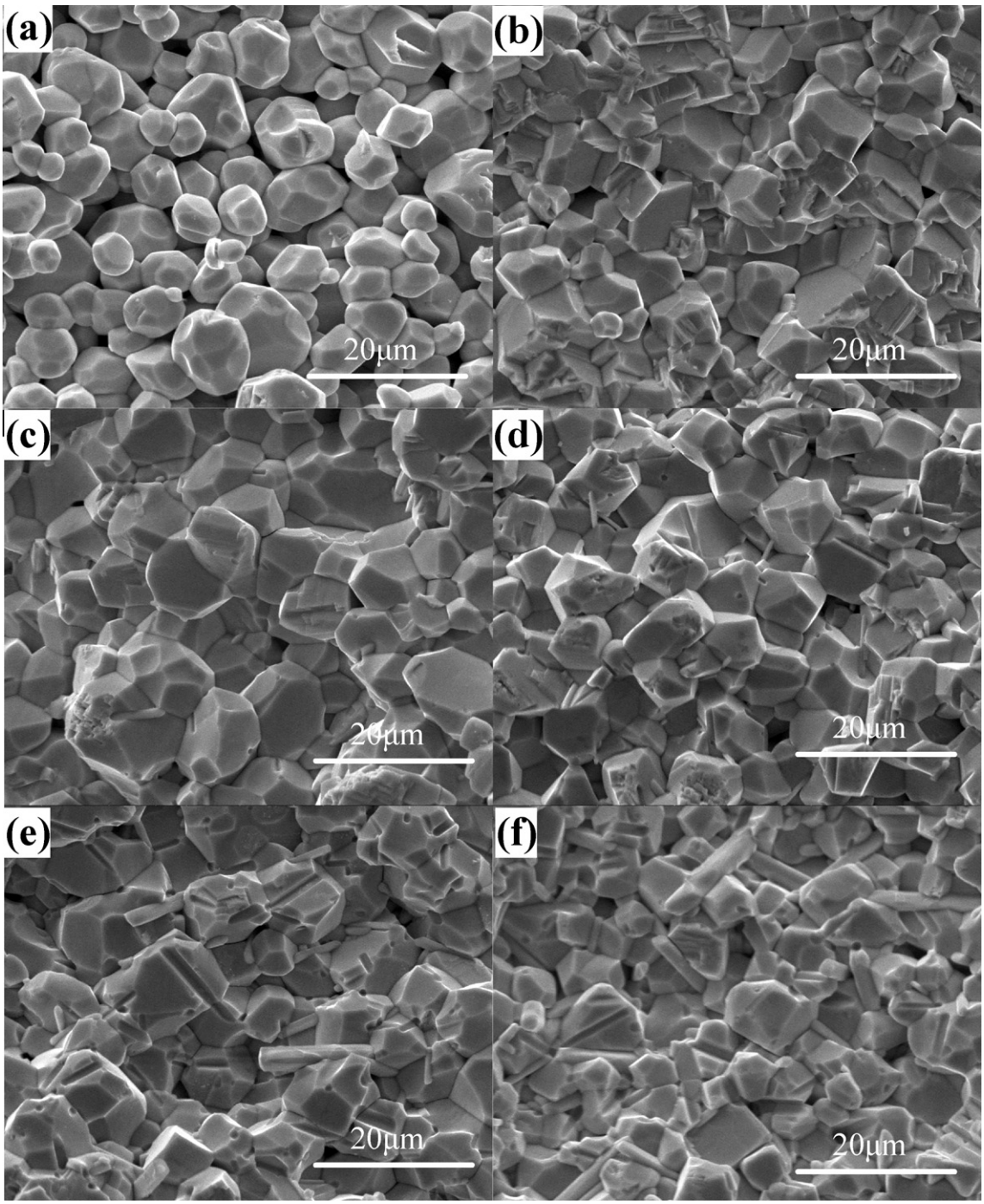

Fig. 3. SEM images of the samples (100−*x*) mol% WO_3 + *x* mol% ZnO: (a) *x* = 0.0; (b) *x* = 0.1; (c) *x* = 0.5; (d) *x* = 1.0; (e) *x* = 5.0; (f) *x* = 10.0.

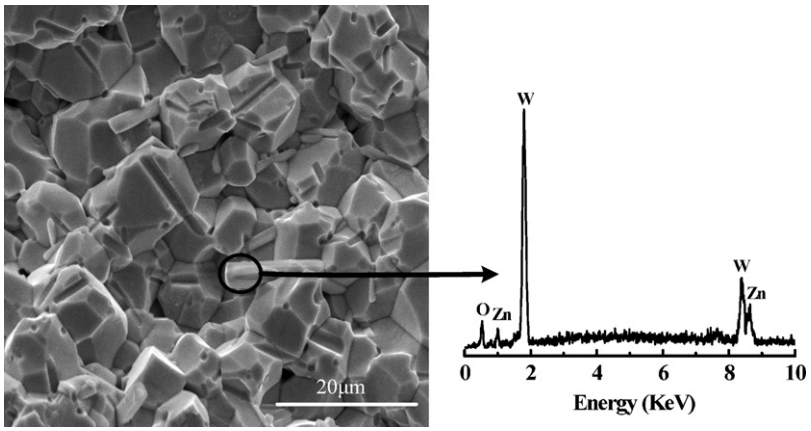

Fig. 4. EDX spectra of grain boundary regions for WO_3 ceramics doped with 5.0 mol% ZnO content.

in Fig. 5. It can be observed that the electrical conductivity of the specimens rises with the increment of ZnO up to 0.5 mol%, and then reduces with adding more ZnO. The electrical conductivity of the sample with 0.5 mol% ZnO is about two orders of magnitude larger than that of the undoped WO_3 in the whole temperature range, and even that of the sample with 10.0 mol% ZnO is still approximately one order of magnitude higher than that of the pure WO_3. Previous studies [31–33] clarified that the electrical properties involving electrical conductivity and thermo-power could not be explained by a simple defects model except under strongly reduced conditions. The electrical conductivity of semiconductors depends on their carrier concentration (n) and mobility (μ) in the following way [34]:

$$\sigma = n\mu e \tag{4}$$

where e is the electron charge. The free-electron concentration in WO_3 is mainly determined by the concentration of defects, such as oxygen vacancies [35]. The electronic structure of the idealized WO_3 indicates [36] that the valence band is dominated by O 2p-like states while the conduction band is determined mainly by the W 5d-like states. The valence state of W can be calculated using the bond valence sum formula reported by Brown and Altermatt [37]. The variations of the average W–O distance and the valence state of W ion with the content of Zn are shown in Fig. 6. For low Zn contents ($x \leq 1.0$ mol%), the increase in the average W–O distance is correlated to the decrease in the valence state of W cation with the increasing content of Zn. Beyond $x = 1.0$ mol%, both of them are almost stable. Recent study [38] reveals that the whole range of W formal oxidation states, from 6+ to 4+, is observed depending on the –W–O–W– chain direction along which the vacancy is created, indicating that the variation in the distance of W–O and in the charge state of W ion is associated with the oxygen vacancies. It can be concluded that the oxygen vacancy increases with the decrease in the valence state of W cation. For larger oxygen vacancy concentrations, the electronic structure is modified [38], and the electrical conductivity is improved. Besides, the mobility of the carriers is strongly influenced by the disorder present in the materials and by impurity doping [34]. The conductivity of WO_3 was reported to decrease due to an increasing volume of the grain boundaries, which contributes to more trapping and scattering of free charge carriers. Therefore, the electrical conductivity of the doped samples in this work could be illustrated by the following competing factors: (1) Zn doping leads to an increment of the grain size and the densification, which increases the relaxation time of electron carriers, and thus raises the electrical conductivity; (2) Substitution of Zn^{2+} for W^{6+} leads to a decrement of the electron concentration and a decrease of the electrical conductivity; (3) The oxygen vacancies increase the electron carrier density as well the electrical conductivity. Factor 2 leads to the decrease of the electrical conductivity, however, factor 1 and factor 3 enhance the electrical conductivity. Hence, the electrical conductivity of the ceramics is modified by the addition of ZnO. The second phase $ZnWO_4$ segregates to the grain boundaries, blocks the migration of the carriers, and thus reduces the electrical conductivity with adding more ZnO.

Fig. 7 presents the Seebeck coefficients (s) for all samples at different temperatures. The absolute value of the s increases with the increment of the temperature, and the Seebeck coefficient values are all negative over the whole temperature range, indicating an n-type conduction. Moreover, the absolute value of the s of the pure WO_3 is a lot larger than our previous work due to the smaller

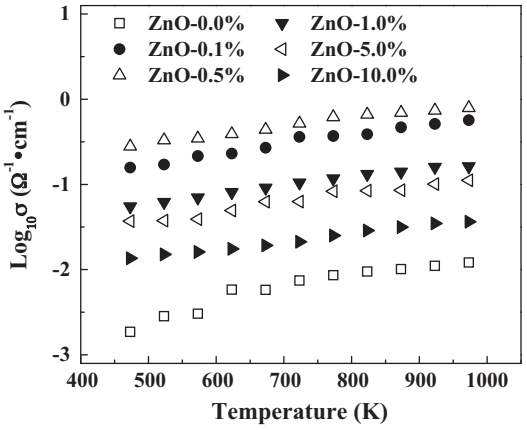

Fig. 5. Temperature dependence of the electrical conductivity of the samples with different amount of ZnO.

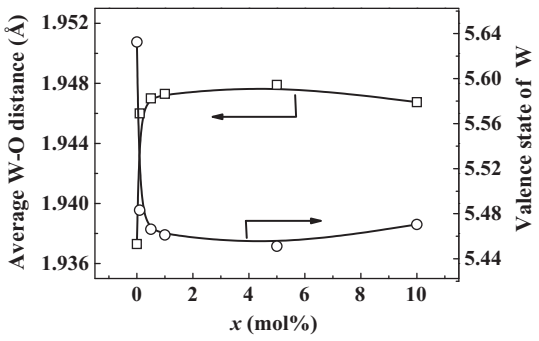

Fig. 6. Average W–O distance and valence state of W ion plotted in terms of ZnO additive concentrations.

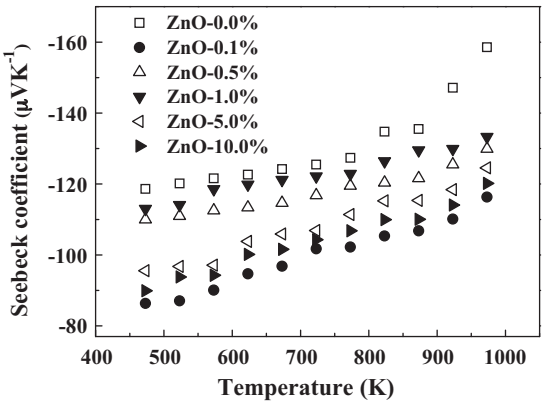

Fig. 7. Temperature dependence of the Seebeck coefficient of the samples with different amount of ZnO.

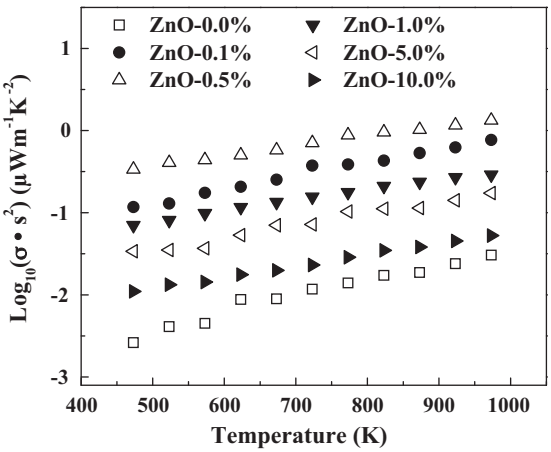

Fig. 8. Temperature dependence of the power factor of Zn doped WO_3 and WO_3 samples.

grain size [24]. The Seebeck coefficient of the undoped WO_3 in this research is almost five times larger than the data reported in our last paper due to the difference of the sintering processes. Recent paper reported by Bérardan et al. [5] demonstrated that the thermoelectric properties of ZnO-based thermoelectric materials were controversial, even the same material at the same temperature with a large discrepancy of the reported data from one team to another, and that their thermoelectric properties appeared to depend strongly on the synthesis conditions. Therefore, it can be concluded that the preparation conditions also have influences on the thermoelectric properties of WO_3-based ceramics, which is essential to further investigate in our next work. According to a simplified broadband model [6,8], the Seebeck coefficient of the n-type semiconductors can be expressed as the following equation:

$$\alpha = -\left(\frac{k}{e}\right)\left[\ln\left(\frac{N_v}{n}\right) + A\right] \quad (5)$$

where k is the Boltzmann constant, n is the electron concentration, e is the electric charge of the carrier, N_v is the density of state, and A is a transport constant, typically $0 \le A \le 2$. In this rule, the Seebeck coefficient decreases with increasing electrical conductivity because of the increment of the electron concentration. Therefore, the Seebeck coefficient of the doped samples is lower than that of the undoped one. Nevertheless, it can be also seen in Fig. 7 that the absolute value of the Seebeck coefficient of the sample with 0.5 mol%, which should be the smallest if the sample followed that rule, is better than that of the sample with 0.1, 5.0 and 10.0 mol%. Moreover, the Seebeck coefficient of the silicon-on-insulator layers reported by Lkeda and Salleh [39] also exhibits unusual behavior and increases with the increasing carrier concentration. The same mechanism is also found in the ZnO thermoelectric materials with the Sb addition [8]. Therefore, the conduction mechanism in the WO_3 ceramics doped with ZnO cannot be explained by a conventional model based on band theory. Additionally, the grain size and the porosity of the ceramics have pronounced effects on the thermoelectric properties [24,25]. As described above, the densification of the sample with 0.5 mol% ZnO is better than other doped specimens, and the Seebeck coefficient of the sample with 0.5 mol% ZnO is also better than that of the sample with 0.1, 5.0 and 10.0 mol%. Moreover, the appearance of the secondary phase usually exhibits positive Seebeck coefficient of $\sim 100\ \mu V\ K^{-1}$ [40]. With the increase of the porosity and $ZnWO_4$, the Seebeck coefficient of the doped samples decreases, and thus the variation of Seebeck coefficient can be explained by the differences of the grain size and porosity.

The thermoelectric power factor (σs^2) of all specimens, calculated from the data in Figs. 5 and 7, as a function of temperature is illustrated in Fig. 8. Since the electrical conductivity of the samples is enhanced enormously, the power factor of WO_3-based ceramics is considerably improved by the addition of ZnO and increases with the temperature rising. As the foregoing discussion, the addition of Zn to WO_3 enhances the electrical conductivity by two orders of magnitude. The sample containing 0.5 mol% ZnO obtains the largest power factor, with a value of $1.34\ \mu W\ m^{-1}\ K^{-2}$ at 973 K, which is approximately three orders of magnitude larger than the data reported in our last paper [24]. However, the power factor of the thermoelectric materials used in current devices is required to have an order of magnitude of $\sim 10^{-4}\ W\ m^{-1}\ K^{-2}$ [41], and the power factor of the WO_3-based ceramics is only one percent of the requirement. The low thermoelectric generation of the WO_3-based ceramics is mainly attributed to the poor electrical conductivity in comparison with other thermoelectric materials, and the electrical conductivity of the pure WO_3 in this study is $0.01\ \Omega^{-1}\ cm^{-1}$ even at 973 K. Therefore, it is significant to uplift the electrical conductivity of the WO_3 ceramics in order to obtain better thermoelectric properties. It has been found that the conductivity of WO_3 can be enhanced by a factor of 10^4 through the addition of Al_2O_3 [42]. Other metal oxide dopants such as Co_3O_4, MnO_2, LiO_2 [17] and TiO_2 [43] have been also observed to elevate the electrical conductivity of WO_3. Hua et al. [22] demonstrated that the quenched WO_3 ceramics exhibited a very low resistivity with a value of 1.95 Ω cm at room temperature, that is to say, a very high conductivity with a value of $0.5\ \Omega^{-1}\ cm^{-1}$ in WO_3 materials. Hence, it is attractive to research the thermoelectric properties of WO_3, because it can be improved by using oxide dopants in addition to WO_3 or by quenching the WO_3 based ceramics.

4. Conclusions

The thermoelectric properties of WO_3 ceramics with the addition of ZnO have been investigated. The results demonstrate that doping ZnO can promote the grain growth and inhibit the porosity. The addition of Zn into WO_3 tremendously improves the electrical conductivity of the WO_3 ceramics by about two orders of magnitude. The densification mechanism and the enhanced electrical conductance principle are opposite to some extent. Thus the electrical properties involving electrical conductivity and thermo-power cannot be explained by a simple defects model. Although the Seebeck coefficient of the samples is slightly reduced, the electrical conductivity of the ceramics is enormously uplifted by doping ZnO. Therefore, the power factor of the samples is enhanced by the addition of ZnO and is about three orders of magnitude higher than our previous work. The second phase $ZnWO_4$ presents in the samples when the dopant concentration of Zn exceeds 1.0 mol%, segregating between the WO_3 grains and making the densification worse. The

grain size decreases and the porosity increases due to the second phase, which degrades the electrical conductivity and the Seebeck coefficient. Therefore, the optimum doping concentration of ZnO in WO_3 is 0.5 mol% that enables the ceramics to have a better thermoelectric property.

Acknowledgment

This work was supported by the National Natural Science Foundation of China under Grant No. 50772092.

References

[1] I. Terasaki, Y. Sasago, K. Uchinokura, Phys. Rev. B 56 (1997) R12685.
[2] K. Park, K.U. Jang, H.C. Kwon, J.G. Kim, W.S. Cho, J. Alloys Compd. 419 (2006) 213.
[3] A.J. Zhou, T.J. Zhu, X.B. Zhao, H.Y. Chen, E. Müller, J. Alloys Compd. 449 (2008) 105.
[4] F. Li, J.F. Li, Ceram. Int. 37 (2011) 105.
[5] D. Bérardan, C. Byl, N. Dragoe, J. Am. Ceram. Soc. 93 (2010) 2352.
[6] S. Teehan, H. Efstathiadis, P. Haldar, J. Alloys Compd. 509 (2011) 1094.
[7] K.P. Ong, D.J. Singh, P. Wu, Phys. Rev. B 83 (2011) 115110.
[8] K. Park, J.K. Seong, S. Nahm, J. Alloys Compd. 455 (2008) 331.
[9] K. Park, J.K. Seong, G.H. Kim, J. Alloys Compd. 473 (2009) 423.
[10] H. Ohta, K. Sugiura, K. Koumoto, Inorg. Chem. 47 (2008) 8429.
[11] M. Ito, T. Matsuda, J. Alloys Compd. 477 (2009) 473.
[12] N. Wang, L. Han, H. He, Y. Ba, K. Koumoto, J. Alloys Compd. 497 (2010) 308.
[13] N. Wang, H. He, X. Li, L. Han, C. Zhang, J. Alloys Compd. 506 (2010) 293.
[14] H.C. Wang, C.L. Wang, W.B. Sun, J. Liu, Y. Sun, H. Peng, L.M. Mei, J. Am. Ceram. Soc. 94 (2011) 838.
[15] H. Kitagawa, T. Kunisada, Y. Yamada, S. Kubo, J. Alloys Compd. 508 (2010) 582.
[16] S.Y. Jung, T.J. Ha, W.S. Seo, Y.S. Lim, S. Shin, H.H. Cho, H.H. Park, J. Electron. Mater. 40 (2011) 652.
[17] S. Yanagiya, N.V. Nong, J. Xu, M. Sonne, N. Pryds, J. Electron. Mater. 40 (2011) 674.
[18] P.S. Patil, P.R. Patil, E.A. Ennaoui, Thin Solid Films 370 (2000) 38.
[19] R.D. Bringans, H. Höchst, H.R. Shanks, Phys. Rev. B 24 (1981) 3481.
[20] A. Yan, C. Xie, D. Zeng, S. Cai, H. Li, J. Alloys Compd. 495 (2010) 88.
[21] Z. Hua, Y. Wang, H. Wang, L. Dong, Sens. Actuators B 150 (2010) 588.
[22] Z. Hua, L. Dong, H. Wang, S. Peng, Y. Wang, Phys. B 406 (2011) 2807.
[23] H. Wang, S. Peng, Z. Hua, X. Dong, Y. Wang, L. Dong, Phys. B 406 (2011) 4183.
[24] H. Wang, Z. Hua, S. Peng, X. Dong, L. Dong, Y. Wang, Ceram. Int. 38 (2012) 1133.
[25] Y.W. Gao, Y.Z. He, L.L. Zhu, Chin. Sci. Bull. 55 (2010) 16.
[26] J.C. Wurst, J.A. Nelson, J. Am. Ceram. Soc. 55 (1996) 109.
[27] X. Chen, D. Chen, P. Lv, F. Yan, Z. Zhan, B. Li, F. Huang, J. Liang, J. Alloys Compd. 476 (2009) 241.
[28] H.M. Rietveld, Acta Crystallogr. 22 (1967) 151.
[29] B.D. Ngom, M. Chaker, N. Manyala, B. Lo, M. Maaza, A.C. Beye, Appl. Surf. Sci. 257 (2011) 6226.
[30] J.A. Cerri, E.R. Leite, D. Gouvêa, E. Longo, J.A. Varela, J. Am. Ceram. Soc. 79 (1996) 799.
[31] P.R. Bueno, E.R. Leite, L.O.S. Bulhões, E. Longo, C.O. Paiva-Santos, J. Eur. Ceram. Soc. 23 (2003) 887.
[32] J. Fayat, M.S. Castro, J. Eur. Ceram. Soc. 23 (2003) 1585.
[33] J. Nowotny, M. Radecka, M. Rekas, J. Phys. Chem. Solids 58 (1997) 927.
[34] M. Regragui, V. Jousseaume, M. Addou, A. Outzourhit, J.C. Bernede, B. El Idrissi, Thin Solid Films 397 (2001) 238.
[35] K. Aguir, C. Lemire, D.B.B. Lollman, Sens. Actuators B 84 (2002) 1.
[36] M. Gillet, K. Aguir, C. Lemire, E. Gillet, K. Schierbaum, Thin Solid Films 467 (2004) 239.
[37] I.D. Brown, D. Altermatt, Acta Crystallogr. B 41 (1985) 244.
[38] F. Wang, C.D. Valentin, G. Pacchioni, Phys. Rev. B 84 (2011) 073103.
[39] H. Lkeda, F. Salleh, Appl. Phys. Lett. 96 (2010) 012106.
[40] W. Shin, N. Murayama, Mater. Lett. 45 (2000) 302.
[41] T. Maekawa, K. Kurosaki, H. Muta, M. Uno, S. Yamanaka, J. Alloys Compd. 387 (2005) 56.
[42] V.O. Makarov, M. Trontelj, J. Eur. Ceram. Soc. 16 (1996) 791.
[43] P.S. Patil, S.H. Mujawar, A.L. Inamdar, P.S. Shinde, H.P. Deshmukh, S.B. Sadale, Appl. Surf. Sci. 252 (2005) 1643.